RESEARCH ARTICLE OPEN ACCESS

Aerodynamic Modelling, Stability Assessment and Low-Cost Fabrication Planning of a NACA 2412 Fixed-Wing UAV Glider Using XFLR5

Kolasani Karthikeya, Jonnala Saicharan, Irfan, Karan Kumar
Department of Computer Science and Engineering
Hyderabad Institute of Technology and Management, Hyderabad, Telangana, India
Corresponding author: kolasanichowdary06@gmail.com
Guide: Mr. T. Raghavendra Gupta, Associate Professor, Department of CSE

----------**********----------

Abstract:

Small unmanned aerial vehicles (UAVs) operate at low Reynolds numbers, where the choice of airfoil, the wing loading and the sizing of the tail surfaces govern both stability and stall behaviour. Evaluating these influences on a computer before any material is cut reduces waste, effort and expense. This paper describes the aerodynamic design and analysis of an inexpensive, hand-launched fixed-wing glider UAV intended for a cruise speed of 10 m/s. The airframe combines a NACA 2412 airfoil, a tapered wing with a 2.0 m span (root chord 0.180 m, tip chord 0.110 m, planform area 0.290 m^2, aspect ratio 13.79), a conventional elevator and a fin. The section was studied in XFoil, and the complete aircraft in XFLR5 v6.62 with the vortex lattice method (VLM1) over angles of attack from −5° to 15°. Analytical calculations based on an assumed mass of 0.45 kg give a wing loading of 15.2 N/m^2, a stall speed between 4.2 and 4.5 m/s, a mean aerodynamic chord of 0.148 m and a cruise Reynolds number near 100,000. The pitching-moment slope is negative, which indicates static stability in pitch, and the spanwise lift distribution is dome-shaped and close to elliptical. The horizontal tail volume coefficient (0.49) lies within the recommended band, whereas the vertical tail volume coefficient (0.013) falls short of the target, so an enlargement of the fin by about 50 % is proposed. Because the analysis is inviscid, drag-related values are indicative only. A low-cost foamboard construction procedure, a centre-of-gravity (CG) balancing method and a flight-test plan are also documented; building and flight-test validation remain pending.

Keywords — **Fixed-wing UAV, glider, NACA 2412, XFLR5, XFoil, vortex lattice method, static stability, wing loading, foamboard construction, low-Reynolds-number aerodynamics.**

----------**********----------

I. Introduction

Unmanned aerial vehicles (UAVs) are now common in surveillance, aerial monitoring, mapping, agriculture and research. How stable, efficient and controllable such a vehicle turns out to be is determined largely by the aerodynamic design of its airframe. The fixed-wing glider is among the simplest UAV layouts: lacking any propulsion, it depends entirely on its wing to turn launch speed and altitude into sustained, steady flight. It is therefore a convenient test case for studying wing design, stability and low-speed aerodynamics.

Small UAVs fly at low Reynolds numbers, where the boundary layer behaves quite differently from that on full-scale aircraft [1]. Airfoil selection, wing loading and tail sizing consequently have a pronounced effect on stall behaviour and stability, and simulating a design before it is built conserves material, time and money. XFLR5 is an analysis package for airfoils, wings and complete aircraft at low Reynolds numbers; it couples the XFoil viscous airfoil solver with lifting-line, vortex-lattice and three-dimensional panel methods [2], [3].

The glider presented here is built around the NACA 2412, a cambered four-digit section that provides good lift at low speed with a gentle stall and is widely used on small UAVs and model aircraft [4]. The airfoil is evaluated with XFoil, and the whole aircraft is evaluated with the vortex lattice method (VLM1) at a flight speed of 10 m/s. These results are backed by hand calculations and by a low-cost foamboard fabrication plan, so that the design can subsequently be built and flight-tested.

A. Motivation

Student teams frequently build first and correct afterwards, which is wasteful; an undersized tail or an aft-placed CG is typically found only after a failed launch. Running the analysis in software first lets the lift distribution, pitch stability and principal design parameters be checked before any material is cut. The goal is an inexpensive and well-documented path from a design concept to a flyable airframe.

B. Problem Statement and Design Targets

A light, slow-flying glider has to be stable, easy to launch by hand and efficient in gliding flight, yet these qualities are hard to judge from construction alone. The problem tackled

 ©IJSRED: All Rights are Reserved

here is the lack of a single documented workflow that leads from performance targets, through airfoil and wing modelling, tail sizing, full-aircraft analysis and hand verification, to a buildable fabrication and test plan. The design follows the targets listed in Table I: a 2.0 m span to balance portability against efficiency, an all-up weight under 600 g to keep the wing loading low, and a stall speed below 6 m/s so that a hand-launched aircraft can recover safely.

TABLE I
PERFORMANCE TARGETS FOR THE GLIDER

Parameter	Target	Notes
Cruise speed	10 m/s	Matches XFLR5 analysis speed
Stall speed	< 6 m/s	Safe hand-launch recovery
Glide ratio (L/D)	> 10:1	Acceptable for a training glider
Wingspan	2.0 m	Portability versus efficiency
All-up weight	< 600 g	Keeps wing loading low
Static margin	5–15 % MAC	Positive, not over-stable

C. Contributions

This paper contributes the following: (i) an integrated design-and-analysis workflow for a 2.0 m foamboard glider; (ii) XFoil and VLM1 results, together with independent hand verification of wing area, aspect ratio, taper ratio, mean aerodynamic chord (MAC), wing loading, stall speed and Reynolds number; (iii) a tail-sizing check that exposes an undersized fin and quantifies the enlargement needed; (iv) an evaluation of the CG position and static margin; and (v) a documented fabrication, balancing and flight-test plan with explicit predictions against which the finished aircraft can be judged. The paper also states clearly which results are inviscid predictions and which validation steps are still outstanding.

II. LITERATURE REVIEW AND BACKGROUND

The design and analysis of small UAV wings rests on established aerodynamic theory and on software that implements it. This section outlines the standard methods employed in the project; it does not report new experimental research.

A. NACA Four-Digit Airfoils

In a four-digit NACA section the first digit specifies the maximum camber as a percentage of chord, the second gives the chordwise position of that camber in tenths of chord, and the final two digits give the maximum thickness as a percentage of chord [4]. The NACA 2412 thus has 2 % camber located at 40 % chord and a thickness of 12 %. The camber yields useful lift even at zero angle of attack, and the moderate thickness produces a progressive stall, a desirable trait for a hand-launched glider.

B. XFoil and Low-Reynolds-Number Effects

XFoil is a panel-method code with a coupled boundary-layer model, developed for airfoils at low Reynolds numbers [3]. Because XFLR5 embeds XFoil, the lift, drag and moment coefficients (C_L, C_D, C_m) of a section can be generated across a range of angles of attack. The transition parameter N_{crit} represents free-stream turbulence, and a value of 9 is the usual setting for ordinary conditions. At Reynolds numbers of about 100,000, a laminar separation bubble may develop on the upper surface of a cambered airfoil, increasing drag and lowering the maximum lift coefficient compared with higher-Reynolds-number data [5]. The local Reynolds number also decreases along a tapered wing toward the tip, where the chord is smallest, so the tip is the likeliest place for early separation.

C. Vortex Lattice Method

The vortex lattice method (VLM) models a lifting surface as a lattice of vortex elements and solves for the circulation that satisfies the flow-tangency condition on every panel [6]. At modest computational cost it provides the lift distribution, induced angle and stability derivatives of a complete aircraft. VLM1 in XFLR5 is accurate within the linear range of angle of attack but cannot be trusted near stall, since it does not represent flow separation.

D. Tail Volume Coefficients and Static Stability

The horizontal and vertical tails are commonly checked through the tail volume coefficients $V_H = S_t L_t/(S \cdot MAC)$ and $V_V = S_v L_v/(S \cdot b)$ [7]. These dimensionless quantities relate tail area and moment arm to wing size and are used at the design stage to judge pitch and yaw stability. An aircraft is statically stable in pitch when a disturbance in angle of attack generates a pitching moment that opposes it; this requires a negative slope of C_m against α together with a CG ahead of the neutral point [8]. The separation between the two, expressed as a fraction of the MAC, is the static margin. A larger margin makes the aircraft more docile but needs more elevator deflection to trim, whereas a very small margin leaves little tolerance for CG errors made during construction [7].

E. Armin-Style Foamboard Construction

The Armin wing is a popular hobbyist technique in which a cambered wing is formed from one flat sheet of foamboard by scoring, folding and gluing it around an internal spar [9]. It requires only a ruler, a craft knife and hot-melt glue, and it reproduces a true airfoil cross-section at very low cost, which suits a student-built glider. Table II summarises the analysis methods used and the role each plays in this work.

TABLE II
COMPARISON OF ANALYSIS METHODS

Method	Typical use	Limitation	Role here
XFoil	2D airfoil C_L, C_D, C_m polars	2D only; poor convergence past stall	NACA 2412 analysis
VLM1	Lift distribution and stability of the full plane	Less accurate near stall; inviscid	10 m/s plane analysis
VLM2	Ring-vortex full-plane analysis	Inviscid in basic form	In project file; not reported
Hand calc.	Check of S, AR, λ, MAC, WL, V_s, Re	Simplified; assumed weight and $C_{L,max}$	Verifies XFLR5 values

 ©IJSRED: All Rights are Reserved

F. Research Gap

The material reviewed treats airfoil selection, planform modelling, tail sizing, stability checks and low-cost construction as separate subjects. For a student team the practical difficulty lies in joining these steps into a single, understandable workflow that ends in a buildable aircraft and an explicit validation plan. Small UAVs also face recurring problems: airfoil performance is sensitive at low Reynolds numbers, a long tapered wing must keep a smooth lift distribution and avoid tip stall, pitch and yaw stability depend on correct tail sizing and CG location, and the airframe has to stay light so that the stall speed remains low. The present work addresses this gap for a 2.0 m foamboard glider.

III. Objectives, Scope and Assumptions

The primary objective is to design, analyse and prepare for fabrication a stable and efficient low-speed glider using XFLR5. The specific objectives are: (i) to design a UAV wing around the NACA 2412 airfoil; (ii) to model the wing, elevator and fin in XFLR5; (iii) to carry out a VLM1 analysis at 10 m/s for angles of attack from −5° to 15°; (iv) to evaluate the lift, drag and pitching-moment characteristics and the spanwise distributions; (v) to verify the main design parameters by hand calculation; and (vi) to document the foamboard fabrication, CG balancing and flight-test plan.

A. Concept of Operations

The aircraft is meant for low-altitude surveillance, aerial monitoring, mapping and data collection [10]. The prototype considered here is a hand-launched, low-speed glider cruising at about 10 m/s. The expected flight profile consists of pre-flight checks, launch, cruise or glide over the mission area, data collection, return to the launch area and a safe landing. The main components are the wing, fuselage, elevator and fin.

B. Out of Scope

A powered mission aircraft would additionally require a propulsion system, flight controller, battery, communication module and ground control station. These items are not part of the unpowered glider analysed here and are regarded as future extensions. The work likewise excludes a viscous full-plane analysis, a built prototype and flight-test data.

C. Assumptions and Constraints

Two quantities in the hand calculations are assumptions rather than measurements. The first is the all-up mass of 0.45 kg, which lies inside the 600 g target. The second is the maximum lift coefficient $C_{L,max}$ = 1.4, a reasonable figure for a cambered low-speed section with a gentle stall, although higher than the value of about 1.2 read from the XFoil graph at Re = 170,000. Both are carried explicitly through the paper and examined in the sensitivity study of Section VI-D. The aircraft is assumed to fly in still air at sea-level density with ground effect off, and the foamboard wing is assumed stiff enough for aeroelastic deformation to be ignored. This last assumption is the weakest for a wing this slender, and it is one reason why the flight test is essential.

The design constraints follow from the intended use. The airframe must be light enough to launch by hand, small enough to transport, simple enough to cut and glue with hand tools, and cheap enough to rebuild after a hard landing. These constraints favour a conventional layout with a straight tapered wing, a single carbon-fibre spar and flat-plate tail surfaces.

IV. Methodology

No machine-learning dataset is used. The inputs to the analysis are design parameters taken from the concept of operations, the project guide [9] and the XFLR5 project file [11] (Table III). The aircraft mass and $C_{L,max}$ are design assumptions and must be confirmed after the glider has been built and tested.

TABLE III
DESIGN INPUT PARAMETERS

Input parameter	Value	Source / remark
Cruise speed	10 m/s	Concept of operations / XFLR5 setup
Airfoil	NACA 2412	Main wing
Wingspan	2.0 m	XFLR5 wing model
Root / tip chord	0.180 m / 0.110 m	XFLR5 wing model
Dihedral	3°	Project guide
Air density	1.225 kg/m^3	Standard sea level
Dynamic viscosity	1.81×10^{-5} kg/(m·s)	Standard air
Assumed all-up mass	0.45 kg	Assumption
Assumed $C_{L,max}$	1.4	Assumption

A. Design Workflow

The workflow opens with the concept of operations, which fixes the mission and performance targets. The NACA 2412 airfoil is analysed in XFoil, the wing is modelled in XFLR5 with the chosen planform, and the elevator and fin are added to complete the aircraft. A fixed-speed VLM1 analysis at 10 m/s is then run for angles of attack from −5° to 15°, and the spanwise distributions and polar graphs are interpreted. Hand calculations verify the principal parameters, after which fabrication, CG balancing and flight testing are planned (Fig. 1).

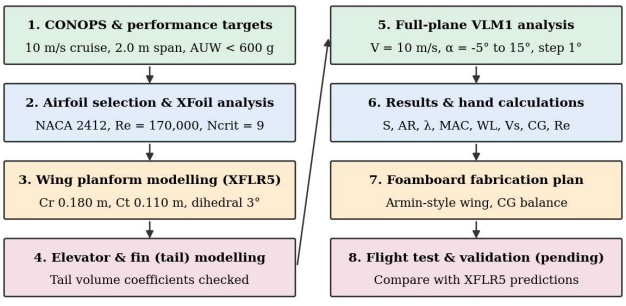


Fig. 1. Proposed design workflow of the UAV fixed-wing glider.

B. Design Equations

The hand calculations used the following relations [12], in which b is the wingspan, C_r and C_t are the root and tip chords,

 ©IJSRED: All Rights are Reserved

W is the weight, ρ is the air density, μ is the dynamic viscosity and V is the flight speed:

$$S = b\,(C_r + C_t)\,/\,2 \quad (1)$$

$$AR = b^2 / S, \quad \lambda = C_t / C_r \quad (2)$$

$$MAC = (2/3)\,C_r\,(1 + \lambda + \lambda^2)\,/\,(1 + \lambda) \quad (3)$$

$$WL = W / S = mg / S \quad (4)$$

$$V_s = \sqrt{[\,2W / (\rho\, S\, C_{L,max})\,]} \quad (5)$$

$$Re = \rho\, V\, MAC / \mu \quad (6)$$

$$X_{CG} = X_{LE,root} + 0.25\, MAC \quad (7)$$

$$V_H = S_t L_t / (S{\cdot}MAC), \quad V_V = S_v L_v / (S{\cdot}b) \quad (8)$$

The wing area sets the lift capacity, and the aspect ratio governs the induced drag. The taper ratio and MAC shape the spanwise loading and fix the reference chord. Wing loading and stall speed determine how slowly and how gently the glider can fly, while the CG position, placed at 25 % of the MAC within an allowed range of 25–33 %, controls pitch stability.

C. Software and Tools

XFLR5 v6.62 was used for airfoil, wing and aircraft design, XFoil (inside XFLR5) for the two-dimensional analysis of the NACA 2412, and VLM1 for the three-dimensional vortex-lattice analysis of the complete aircraft. XFLR5 was run under the Windows operating system.

V. IMPLEMENTATION

A. Airfoil Selection and XFoil Analysis

The NACA 2412 was chosen because it provides good lift at low speed, behaves stably and is in common use in UAV applications. It was generated within XFLR5 (Fig. 2) and analysed in XFoil with the settings of Table IV.

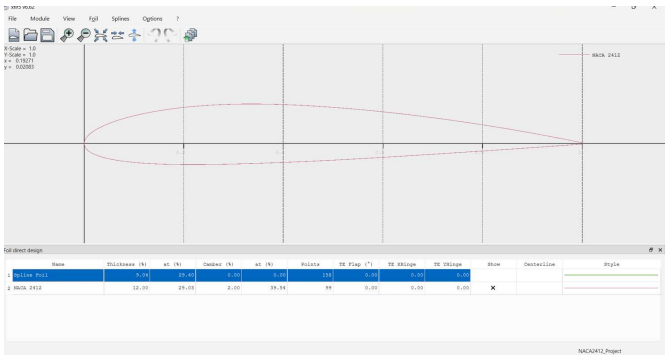


Fig. 2. NACA 2412 airfoil generated in XFLR5.

TABLE IV
XFOIL SETTINGS FOR THE NACA 2412

Setting	Value
Analysis type	Type 1 (fixed speed)
Reynolds number	170,000
Mach number	0.03
N_{crit}	9
Angle-of-attack sweep	−5° to 15°, step 0.5°
Initialise boundary layer	Enabled

The results window (Fig. 3) presents the C_D–C_L polar, the C_L–α curve, the C_m–α curve and the transition and hinge-moment plots. The lift coefficient rises almost linearly with angle of attack and starts to level off at about 1.2 near the upper end of the sweep, the minimum drag coefficient is of the order of 0.01, and the pitching-moment coefficient stays negative over most of the range. These values are read from the graphs and are approximate.

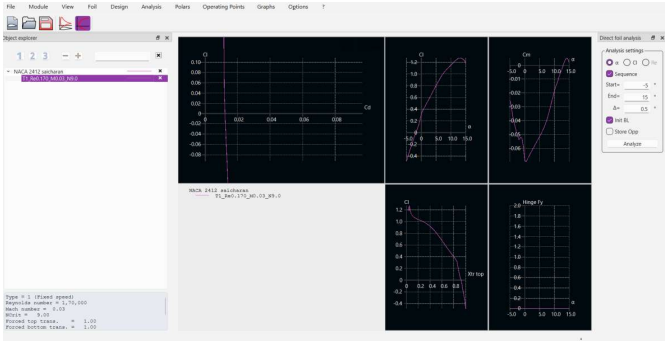


Fig. 3. XFoil analysis of the NACA 2412 airfoil.

B. Wing Planform Modelling

The wing was modelled in XFLR5 as a tapered wing with a root and a tip section, both using the NACA 2412. XFLR5 models a single half-wing and mirrors it, so the total span is twice the 1.0 m half-span. The section geometry is listed in Table V and the planform is shown in Fig. 4. XFLR5 reports a span of 2.000 m, a wing area of 0.290 m^2, a MAC of 0.148 m, an aspect ratio of 13.793 and a taper ratio of 0.611, all of which agree with the hand calculations.

TABLE V
WING SECTION GEOMETRY

Section	y (m)	Chord (m)	Offset (m)	Dihedral	Twist
Root	0.000	0.180	0.000	3.0°	0.0°
Tip	1.000	0.110	0.018	3.0°	0.0°

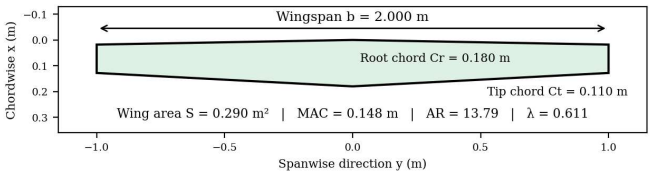


Fig. 4. Wing planform of the UAV glider (generated from the model dimensions).

The planform reflects the mission. An aspect ratio as high as 13.79 keeps induced drag low, which is what a glider needs to convert height into distance. A taper ratio of 0.611 brings the spanwise loading closer to the elliptical ideal than a rectangular wing would, and it lowers structural weight toward the tip, where the bending moment is smallest. The 3° of dihedral supplies inherent roll stability, so that sideslip produces a rolling moment that levels the wings without a rudder or ailerons. The model has no twist; adding a small amount of washout is identified as a later refinement to delay tip stall.

 ©IJSRED: All Rights are Reserved

C. Tail Assembly Design

The elevator (horizontal stabiliser) provides pitch stability and the fin (vertical stabiliser) provides yaw stability. Both surfaces were sized according to the project guide and checked with the tail volume coefficients of Eq. (8) (Table VI). The complete aircraft model is shown in Fig. 5.

TABLE VI
TAIL PARAMETERS AND VOLUME COEFFICIENTS

Parameter	Elevator	Fin
Half-span / height	0.25 m (total 0.50 m)	0.15 m
Root / tip chord	0.08 m / 0.06 m	0.10 m / 0.07 m
Approx. area	$S_t \approx 0.035$ m^2	$S_v \approx 0.013$ m^2
Moment arm	$L_t = 0.60$ m	$L_v = 0.60$ m
Volume coefficient	$V_H \approx 0.49$	$V_V \approx 0.013$
Guide target	0.35–0.55	> 0.02

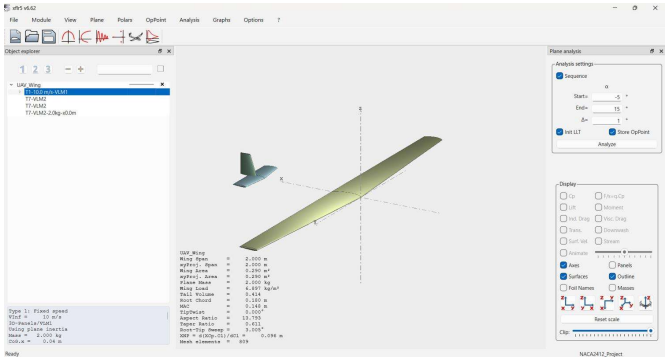


Fig. 5. XFLR5 plane model (wing, elevator and fin) with geometry data.

The horizontal tail volume coefficient ($V_H \approx 0.49$) lies inside the recommended range. The vertical tail volume coefficient ($V_V \approx 0.013$) is below the guide target of 0.02, so the fin has to be enlarged before fabrication (Section VI-E). XFLR5 additionally reports a tail volume of 0.414 based on its own definition. The elevator setting angle is −2°. The project guide recommends a symmetric NACA 0009 section for the tail, but the supplied XFLR5 project file contains only the NACA 2412, which was therefore also used for the elevator and fin.

The tail arms were held at 0.60 m because, for a glider of this size, the fuselage boom is the main structural weight behind the CG: lengthening it improves the volume coefficients but shifts the CG aft unless nose ballast is added. The chosen arm is a compromise between tail effectiveness and boom weight, and enlarging the fin is a cheaper way of raising V_V than lengthening the boom.

D. Full-Plane VLM1 Setup

The complete aircraft was analysed with a fixed-speed VLM1 analysis using the settings of Table VII. The project file holds two runs, a standard run and an inviscid run, and the polar graphs and spanwise plots reported here come from the inviscid run.

TABLE VII
VLM1 ANALYSIS SETTINGS

Setting	Value
Analysis type	Type 1 – fixed speed
Method	3D panels / VLM1
Free-stream speed	10 m/s
Angle-of-attack sweep	−5° to 15°, step 1°
Air density	1.225 kg/m^3
Ground effect	Off
Mass shown in XFLR5	2.000 kg (see Section VIII)
CoG x-position in XFLR5	0.04 m

VI. RESULTS AND DISCUSSION

A. Spanwise Distribution

Fig. 6 plots the induced angle, total angle, local lift coefficient C_l, local lift and airfoil drag for all angles of attack from −5° to 15°. The induced angle varies smoothly along the span and reveals the downwash variation, while the total angle grows with the applied angle of attack. The C_l distribution shows smooth spanwise loading, and the local lift forms a dome-shaped curve broadly resembling an elliptical loading, which is favourable for low induced drag and for avoiding an overloaded tip. The airfoil-drag graph is empty in the inviscid run because viscous drag is not computed; Fig. 7 shows the airfoil drag distribution from the standard VLM1 run, in which the graph does contain data.

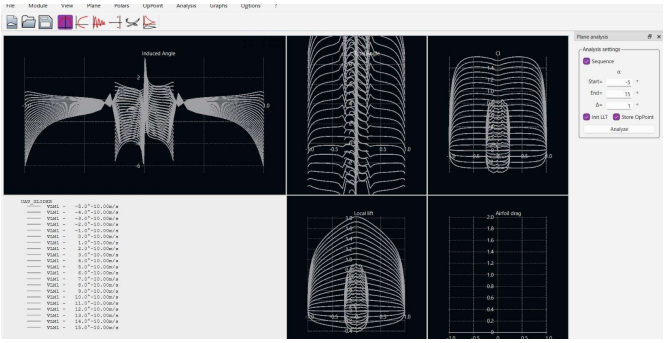


Fig. 6. Plane analysis – induced angle, total angle, C_l, local lift and airfoil drag (inviscid run).

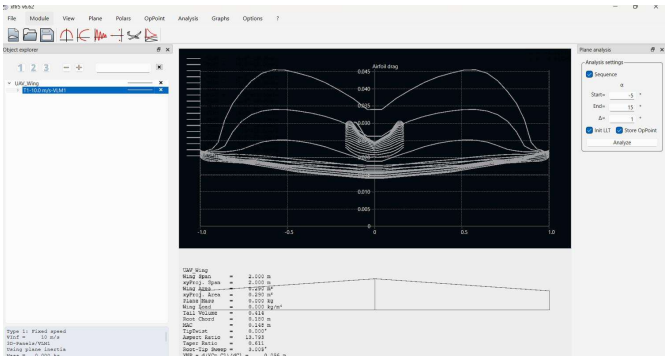


Fig. 7. Airfoil drag distribution from the standard VLM1 run.

B. Aerodynamic Polars

Fig. 8 presents the polar graphs of the complete aircraft from the inviscid VLM1 run: C_L–C_D, C_L–α, C_m–α, C_L/C_D–α and

 ©IJSRED: All Rights are Reserved

the endurance parameter $\sqrt{(C_L^3/C_D^2)}$ against α. The C_L–C_D polar is smooth, with C_L reaching about 1.6 at a C_D of about 0.06. Lift grows almost linearly with angle of attack, with a slope of roughly 5 per radian read from the graph. The C_m–α slope is negative, which indicates longitudinal static stability. C_L/C_D and the endurance parameter peak at low angles of attack and decline as C_L increases.

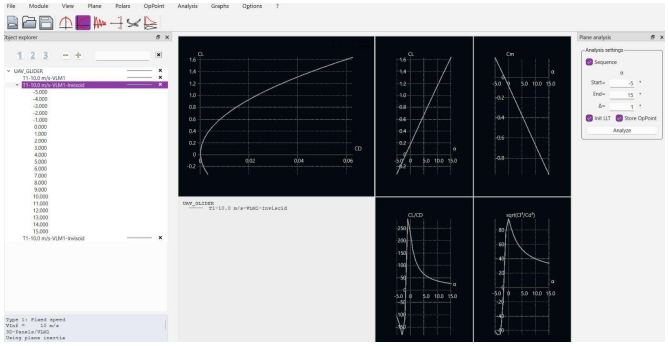


Fig. 8. Aerodynamic polar graphs of the UAV glider (inviscid VLM1).

Since the run is inviscid, the drag consists only of induced drag, so C_L/C_D simply decreases as C_L increases, and its magnitude (above 200 near zero angle of attack and roughly 50–65 at 5–7°) is far higher than a real glider could reach. The best-glide angle of attack and a realistic glide ratio must therefore come from a viscous analysis that includes the XFoil polars. The design target of L/D above 10:1 is expected to be met in practice but has not yet been demonstrated.

Two further features merit comment. First, the C_L–α curve remains straight over the entire analysed range with no sign of a lift break, as expected because VLM1 is linear and does not model separation; the maximum useful lift coefficient of the real aircraft is thus set by the airfoil, as read from the XFoil results, and not by the aircraft analysis. Second, the C_m–α curve is also nearly straight, so the restoring moment builds steadily with angle of attack, which is the behaviour wanted from a hand-launched glider that may leave the hand at a slightly wrong attitude.

C. Design Calculations

The principal design parameters were verified by hand with Eqs. (1)–(8) and are collected in Table VIII. Every wing-geometry value agrees with that reported by XFLR5 (span 2.000 m, area 0.290 m², MAC 0.148 m, AR 13.793, taper 0.611), confirming that the wing was entered correctly in the model.

TABLE VIII
DESIGN CALCULATIONS

Quantity	Substitution	Result
Wing area	2.0 × (0.180 + 0.110)/2	0.290 m²
Aspect ratio	2.0^2 / 0.290	13.79
Taper ratio	0.110 / 0.180	0.611
MAC	(2/3)(0.180)(1 + 0.611 + 0.611^2)/(1 + 0.611)	0.148 m
Wing loading	(0.45 × 9.81)/0.290	15.2 N/m²
Stall speed	√[(2 × 4.41)/(1.225 × 0.290 × 1.4)]	4.2 m/s
CG position	0.25 × 0.148	0.037 m from LE
Reynolds number	1.225 × 10 × 0.148 / 1.81×10^{-5}	≈ 100,000

The wing loading of 15.2 N/m² is well below the 30 N/m² limit adopted for a low-speed glider, and the stall speed of 4.2 m/s is below the 6 m/s target. Substituting the $C_{L,max}$ of about 1.2 read from the XFoil graph for the assumed 1.4 gives a stall speed of about 4.5 m/s, which still satisfies the target.

D. Sensitivity of Wing Loading and Stall Speed

Because the mass and $C_{L,max}$ are assumptions, Eqs. (4) and (5) were evaluated for other plausible values (Table IX), keeping the wing area at 0.290 m² and the air density at 1.225 kg/m³. Even at the upper weight limit of 0.60 kg with $C_{L,max}$ = 1.2, the stall speed remains below the 6 m/s target, so the stall requirement is not sensitive to moderate errors in the mass estimate. The Reynolds number scales linearly with speed, from about 80,000 at 8 m/s to about 120,000 at 12 m/s, so the whole planned flight envelope lies within the same low-Reynolds-number regime.

TABLE IX
SENSITIVITY OF WING LOADING AND STALL SPEED (CALCULATED)

Mass (kg)	WL (N/m²)	V_s at $C_{L,max}$ = 1.4	V_s at $C_{L,max}$ = 1.2
0.45	15.2	4.2 m/s	4.5 m/s
0.50	16.9	4.4 m/s	4.8 m/s
0.60	20.3	4.9 m/s	5.3 m/s

E. Fin Sizing Estimate

The vertical tail volume coefficient of 0.013 is below the guide value of 0.02. Rearranging Eq. (8) for the fin area gives

$$S_v = V_V S b / L_v \quad (9)$$

With S = 0.290 m², b = 2.0 m and the existing moment arm of 0.60 m, reaching V_V = 0.02 requires a fin area of about 0.019 m², roughly 50 % more than the present 0.013 m². Alternatively the moment arm could be lengthened, since for a fixed fin area the coefficient grows in direct proportion to L_v. Either route is inexpensive in foamboard and adds very little weight, so the fin should be enlarged on the cutting template before any material is cut. The horizontal tail needs no change, as the recomputed value $S_tL_t/(S\cdot MAC)$ = 0.035 × 0.60 / (0.290 × 0.148) ≈ 0.49 agrees with Table VI.

F. CG and Stability Evaluation

For pitch stability the CG must lie ahead of the neutral point. The project guide places the CG target at 25–33 % of the MAC (Table X). The pitching-moment coefficient falls steadily as the angle of attack rises, so any pitch disturbance produces a restoring nose-down moment; together with the horizontal tail volume coefficient of about 0.49 and a neutral point behind the modelled CG, this indicates that the glider is statically stable in pitch. The weak point is the vertical tail, whose volume coefficient is below target.

 ©IJSRED: All Rights are Reserved

TABLE X
CG AND STABILITY PARAMETERS

Parameter	Value	Remark
MAC	0.148 m	Hand calc. and XFLR5
CG at 25 % MAC	0.037 m from root LE	Guide target
CG at 33 % MAC	0.049 m from root LE	Aft limit of guide
Neutral point (XFLR5)	0.096 m	As reported by XFLR5
CoG used in XFLR5	0.04 m	Analysis panel
Indicative static margin	≈ 38 % MAC	(0.096 − 0.04)/0.148
Static margin target	5–15 % MAC	Project guide

The indicative static margin is defined as

$$SM = (X_{NP} - X_{CG}) / MAC \quad (10)$$

and its value is larger than the 5–15 % target, meaning the glider is strongly stable and may be less agile. Even at the aft guide limit of 0.049 m the margin would be about 32 % MAC, so the two guide targets (CG at 25–33 % MAC and a margin of 5–15 %) cannot both be met with the present neutral-point value; the final balance point must be set from the full XFLR5 stability analysis. A more aft CG, for example about 0.08 m from the XFLR5 reference point for a margin of roughly 10 %, could then be considered. This is only an indication from the displayed values and must be confirmed in the stability analysis and by a physical balance test. A note on the datum is also needed: Eq. (7) and Table X measure the CG from the root leading edge, as in the project guide, whereas the MAC leading edge lies about 0.008 m aft of it for this taper and sweep offset, so the 25 % MAC point is closer to 0.045 m from the root leading edge. The same datum must be used both when marking the CG on the airframe and when entering it in XFLR5.

G. Comparison with Performance Targets

Table XI sets the predicted values against the targets of Table I. The span and cruise speed are met by construction. The predicted stall speed meets the target with margin, even under the less favourable $C_{L,max}$. The weight target is met only on the basis of the assumed 0.45 kg and must be confirmed by weighing the finished glider. The glide-ratio target cannot yet be confirmed because the only available figures come from the inviscid run, and the static margin lies above the intended band. This presentation separates the targets the design already satisfies from those that depend on pending refinements.

TABLE XI
PREDICTED RESULTS AGAINST PERFORMANCE TARGETS

Parameter	Target	Predicted	Status
Cruise speed	10 m/s	Analysed at 10 m/s	Met
Wingspan	2.0 m	2.000 m	Met
Stall speed	< 6 m/s	4.2–4.5 m/s	Met (predicted)
All-up weight	< 600 g	0.45 kg (assumed)	To be weighed
Glide ratio	> 10:1	Inviscid only	Not yet shown
Static margin	5–15 % MAC	≈ 38 % (indicative)	Above target
V_H / V_V	0.35–0.55 / > 0.02	0.49 / 0.013	V_V below target

VII. FABRICATION AND FLIGHT-TEST PLAN

The glider is planned to be built from 5 mm foamboard using the Armin-style folded-wing method [9]. Table XII lists the materials and the purpose of each. No photographs of a built glider exist at this stage, so this section describes the planned procedure only.

TABLE XII
FABRICATION MATERIALS AND PURPOSE

Material / tool	Specification	Purpose
Foamboard	5 mm, 3 A1 sheets, paper-backed	Wing skins, fuselage, tail
Hot glue gun	High temperature (195 °C+)	Structural joints
Metal ruler	600 mm, not plastic	Straight scoring and cutting
Craft knife	Sharp; blade changed every 3–4 cuts	Clean cuts and scoring
Carbon fibre rod	3 mm diameter, 1 m long	Main spar for bending strength
Packing tape	Clear, 1 roll	LE reinforcement, tape hinges
Sanding block	120 grit	Tapering the trailing edge

A. Construction Sequence

The planned sequence is: (1) cut the bottom skin of each wing half as a trapezoid with a 180 mm root chord, 110 mm tip chord and 1000 mm length; (2) fix the internal foamboard spar at about 25–30 % of the chord and add the carbon-fibre rod; (3) score and fold the leading edge over the spar to form the cambered upper surface and reinforce it with tape; (4) taper the trailing edge by sanding and bond the upper and lower skins; (5) add root and tip ribs, join the two wing halves and set the dihedral to about 3°; and (6) build the fuselage boom, mount the wing and attach the elevator and fin with taped hinges.

Build quality directly determines whether the flight matches the analysis. The two wing halves must be cut from the same template so that they are mirror images, because a difference in area or camber causes a constant rolling tendency. The wing and elevator must be mounted without relative twist, and the −2° elevator setting used in the model should be reproduced with a simple cardboard gauge. Hinge gaps should be sealed with tape, since an open gap leaks air from the high-pressure to the low-pressure side and weakens control effectiveness. The as-built mass and CG position should be recorded after every repair so that the analysis inputs stay consistent with the aircraft actually flown.

B. Balance Check and Flight Test

Before flight, the CG is checked by balancing the glider on two fingertips at the marked CG position; a slight nose-heavy tendency is safe, but a tail-heavy glider must not be flown. The flight test is planned as a chuck-glider test over open grass in light wind, with a slow, a standard (8–10 m/s) and a fast throw,

 ©IJSRED: All Rights are Reserved

recorded on video. Each session begins with a visual inspection of the glue joints, hinges and spar, followed by the finger-balance check. The first throws are gentle, level launches from shoulder height into the wind so that trim can be adjusted by bending the elevator trailing edge in small steps; launch speed is raised toward the 8–10 m/s throw only once the aircraft glides straight and flat. For each throw the observer records the launch type, any stall or pitch-up behaviour, any tendency to roll or yaw, the glide path and the landing distance. The glide angle is estimated from the release height and the distance travelled in the video, giving a rough measured glide ratio. The observed behaviour will be compared with the predictions in Table XIII.

TABLE XIII
PREDICTIONS TO BE COMPARED WITH FLIGHT TESTS

Parameter	Predicted / target	Observed
Stall speed	≈ 4.2 m/s (hand calc.); ≈ 4.5 m/s with $C_{L,max}$ = 1.2	Pending
Glide ratio (L/D)	> 10:1 target; inviscid VLM1 gives 50–65 at 5–7°	Pending
Pitch stability	Stable (negative C_m slope, VLM1)	Pending
CG position	25 % MAC (0.037 m from root LE)	Pending

C. Risks and Safety

A tail-heavy balance is the most dangerous risk and is prevented by the finger-balance check and, if necessary, nose ballast. Tip stall on the slender tapered wing is addressed by gentle launches and, later, by washout. Warping of paper-backed foamboard in humid air alters camber and incidence, so the structure should be stored dry and re-checked before each session. A small fin is likely to give a lazy or oscillatory yaw response, which is a further reason to enlarge it before building.

Although a 0.45 kg hand-launched glider carries little energy, test flights should take place over open ground, away from people, roads and power lines, in light wind and good visibility, with throws directed away from spectators. Regulations for unmanned aircraft differ between countries and may apply even to small models, so the team should check the requirements of the local aviation authority and the institution before any flight and keep the aircraft within visual line of sight.

VIII. LIMITATIONS AND REFINEMENT PLAN

The present status of each stage is given in Table XIV. The following limitations apply to the results. (1) Inviscid analysis: the polar graphs come from an inviscid VLM1 run, so viscous drag is excluded and drag-based figures are indicative only. (2) Mass setting: the XFLR5 panel shows an aircraft mass of 2.000 kg, whereas the hand calculations assume 0.45 kg. (3) Reynolds number: the XFoil analysis used Re = 170,000, whereas the hand calculation gives about 100,000 at 10 m/s. (4) Tail airfoil and fin: the tail uses the NACA 2412 instead of a symmetric section, and the vertical tail volume coefficient is below target. (5) Static margin: the indicative value of about 38 % MAC exceeds the target band. (6) No experimental validation: fabrication, balance and flight-test results are not yet available, so all results are predictions.

TABLE XIV
STATUS OF PROJECT STAGES AND PENDING VALIDATION

Stage	Description	Status
Airfoil analysis	NACA 2412 in XFoil	Completed
Wing modelling	Tapered 2.0 m wing in XFLR5	Completed
Tail modelling	Elevator and fin added	Completed; fin to be enlarged
VLM1 analysis	10 m/s, −5° to 15°	Completed (inviscid)
Hand calculations	S, AR, λ, MAC, WL, V_s, CG, Re	Completed
Fabrication	Foamboard glider	Planned
CG balance test	Finger-balance check	Pending
Flight test	Chuck-glider test and comparison	Pending

These limitations translate into an ordered list of analysis tasks. First, the aircraft mass in XFLR5 should be changed to the measured glider weight and the CG set to the position actually marked on the airframe. Second, the XFoil analysis should be repeated at Re ≈ 100,000 and the resulting polar used in a viscous aircraft analysis so that drag is no longer purely induced. Third, a full XFLR5 stability analysis should be run to obtain the neutral point and static margin of the complete aircraft, replacing the indicative value. Fourth, the enlarged fin and, where available, a symmetric tail section such as the NACA 0009 recommended by the project guide should be modelled and the volume coefficients rechecked. Each step is inexpensive and can be completed before any material is cut, which is the main benefit of the analysis-first approach.

The present results support the following. The geometry checks, the hand calculations and the sign of the pitching-moment slope are robust, since they follow from simple relations and from a method that is accurate in the linear range. The magnitude of the glide ratio, the best-glide angle of attack and the exact static margin are not robust at this stage and should not be quoted as performance claims until the viscous analysis and flight tests are complete.

IX. CONCLUSION AND FUTURE SCOPE

The XFLR5 analysis indicates that the glider with the NACA 2412 airfoil has favourable aerodynamic characteristics for low-speed flight at 10 m/s. The lift distribution is dome-shaped and close to elliptical, lift rises almost linearly with angle of attack, and the negative pitching-moment slope points to longitudinal static stability. The calculated wing loading of 15.2 N/m^2, stall speed of 4.2–4.5 m/s and Reynolds number of about 100,000 are appropriate for a lightweight foamboard UAV. The vertical tail should be enlarged by about 50 % in area, and the mass setting, the Reynolds number of the airfoil analysis and the viscous drag should be refined before the design is considered ready for flight testing.

Future work will repeat the aircraft analysis with viscous XFoil-based polars to obtain the best-glide angle and a realistic L/D, run the XFLR5 stability analysis with the real weight and CG, enlarge the fin, and add washout to delay tip stall. Once the glider is built, balance and flight tests will be compared with

 ©IJSRED: All Rights are Reserved

the predictions in Table XIII. The design could also be extended to a powered version with a propulsion system, flight controller, battery and communication module for surveillance and mapping missions.

The workflow is reusable for any small fixed-wing design: define the mission and targets, select and verify an airfoil, model the planform and tail, run a full-aircraft analysis, check the main parameters by hand, and only then commit material. For students it makes every design decision traceable to a number, so that the eventual comparison between prediction and flight result is far more informative than a simple pass or fail.

ACKNOWLEDGMENT

The authors thank their internal supervisor and guide, Mr. T. Raghavendra Gupta, Associate Professor, Department of CSE, for technical guidance and constant encouragement, and the Program Head and the Hyderabad Institute of Technology and Management for the facilities provided.

REFERENCES

[1] T. J. Mueller and J. D. DeLaurier, "Aerodynamics of small vehicles," *Annual Review of Fluid Mechanics*, vol. 35, pp. 89–111, 2003.

[2] A. Deperrois, *XFLR5 – Analysis of Foils and Wings Operating at Low Reynolds Numbers*, user guide and software documentation (v6.62), www.xflr5.tech.

[3] M. Drela, "XFOIL: An analysis and design system for low Reynolds number airfoils," in *Low Reynolds Number Aerodynamics*, Lecture Notes in Engineering, vol. 54, Springer-Verlag, 1989.

[4] I. H. Abbott and A. E. von Doenhoff, *Theory of Wing Sections, Including a Summary of Airfoil Data*. New York: Dover Publications, 1959.

[5] P. B. S. Lissaman, "Low-Reynolds-number airfoils," *Annual Review of Fluid Mechanics*, vol. 15, pp. 223–239, 1983.

[6] J. Katz and A. Plotkin, *Low-Speed Aerodynamics*, 2nd ed. Cambridge, U.K.: Cambridge University Press, 2001.

[7] D. P. Raymer, *Aircraft Design: A Conceptual Approach*. Reston, VA: AIAA Education Series.

[8] R. C. Nelson, *Flight Stability and Automatic Control*, 2nd ed. New York: McGraw-Hill, 1998.

[9] Project guide, "Design & Analysis of a Custom Fixed-Wing Glider: Complete Step-by-Step Modeling & Construction Guide," supplied with the project files (unpublished).

[10] Project documents: *UAV Wing Analysis Full Report* and *CONOPS (UAV) Report*, team documents (unpublished).

[11] XFLR5 project file NACA2412_Project.xfl, team project file (unpublished).

[12] J. D. Anderson, *Fundamentals of Aerodynamics*. New York: McGraw-Hill Education.

 ©IJSRED: All Rights are Reserved